Case Studies in Thermal Engineering 12 (2018) 38–46

Contents lists available at ScienceDirect

Case Studies in Thermal Engineering

journal homepage: www.elsevier.com/locate/csite

On the conceptual design of the novel balanced rolling piston expander

Antonio Giuffrida[a,*], Gianluca Valenti[a], Davide Palamini[a], Luigi Solazzi[b]

[a] Politecnico di Milano, Dipartimento di Energia, Via Lambruschini 4A, 20156 Milano, Italy
[b] Università degli Studi di Brescia, Dipartimento di Ingegneria Meccanica e Industriale, Via Branze 38, 25123 Brescia, Italy

ARTICLE INFO

Keywords:
Positive-displacement
Expander
Balanced rotor
Rolling piston
Cam-shaped rotor

ABSTRACT

This work presents a novel type of positive-displacement expander, named the balanced rolling piston expander. It proposes also a design procedure and assesses the mechanical behavior of a virtual prototype. The expander is conceptually capable of operating at higher fluid temperatures than other positive-displacement expanders, such as scroll- or screw-type machines. Moreover, it employs a radially balanced rotor, differently from common rolling piston technologies and does not require any timing mechanism for filling and emptying the working chambers, differently from Wankel or reciprocating solutions. The investigated virtual prototype is chosen for the study case of a small-scale heat recovery unit currently under investigation. The results indicate that a prototype of about 300 mm in diameter and 100 mm in length is capable of an ideal power of 20 kW. Moreover, vane accelerations can be relatively high but anyhow comparable to those in sliding vane machines, while pressure drops in percent terms are in general lower than 1%. Lastly, load-induced displacements are manageable by a proper radial clearance at room temperature. In brief, the balanced rolling piston expander is a promising option for small-scale power generation units operating with temperatures not achievable by common technologies and, hence, it deserves further investigation.

1. Introduction

The power generation infrastructure is changing from a system in which electricity used to be produced exclusively in large power plants to a system in which diffused generation and smart grids will be integrated closely with those larger technologies. In such a transition, small-scale power generation units are becoming more and more common. Similarly to the large plants, these small units can be based on a Rankine cycle or a Joule-Brayton cycle. However, the great reduction in the output capacity imposes a fundamental switch in the technology of the fluid machines, which are not mere reduced-scale models. In the small units, positive-displacement expanders must replace generally the turboexpanders of the large plants because of their lower process flow rates and rotational speeds as well as of their ability to operate under large pressure ratios and at good performance [1]. Organic Rankine Cycles (ORCs) offer an example of this technology switch: positive-displacement expanders are employed for units scaled up to tens of kilowatts, whereas turbomachines above a hundred of kilowatts [2].

There exist many types of positive-displacement expanders [1], such as reciprocating, rolling piston, scroll, single- as well as twin-screw, sliding vane, and Wankel. Each type is characterized by a maximum temperature of the working fluid at the machine inlet, as explained in the next section. This maximum temperature can hinder the use of an expander type within small-scale power generation

* Corresponding author.
E-mail address: antonio.giuffrida@polimi.it (A. Giuffrida).
URL: http://www.gecos.polimi.it (A. Giuffrida).

https://doi.org/10.1016/j.csite.2018.03.003
Received 29 September 2017; Received in revised form 23 January 2018; Accepted 7 March 2018
Available online 08 March 2018

units operating at mid and high temperatures.

1.1. Overview on positive-displacement expanders

The open literature provides several studies about diverse types of positive-displacement expanders. An overview is reported here focusing mainly on the maximum temperature of the working fluid at the machine inlet. In particular, the expander types are presented in an increasing order of this temperature.

Thanks to their relatively simple technology, rolling piston expanders are proposed primarily as substitutes of the throttling valves in carbon dioxide heat pumps to improve their coefficient of performance, as indicated by Haiquing et al. [3]. In addition to heat pumps, however, rolling piston expanders are also applied to micro-scale ORC units in which the maximum temperature does not exceeds normally 90 °C, according to Zheng et al. [4].

Sliding vane expanders operating with compressed air are adopted usually to substitute electric motors, for example inside pneumatic tools, in spark-prohibited environments. Although originally sliding vane expanders are not designed to operate with organic fluids, Qiu et al. [5] state they are a good option after proper modifications for power outputs lower than a few kilowatts. Small ORC units employing sliding vane expanders are investigated in a number of works spanning over diverse working fluids and over different maximum temperatures up to about 130 °C [6–11].

There are various studies about the performance of scroll expanders [12–14] or that of ORC units employing them, as reported by Quoilin et al. [15]. The manufactured prototypes are developed usually for laboratory tests by modifying commercial scroll compressors. Their operation is limited now to maximum temperatures not higher than 175 °C [12,16]. Such temperatures are possible in case of open-drive machines, but Lemort et al. [17] highlight that lower maximum temperatures are necessary for hermetic machines in presence of lubricating oil.

Screw expanders shall be distinguished into single- and twin-screw technologies. Among the several researches about the single-screw technology, Desideri et al. [18] characterize experimentally an ORC unit by modifying a single-screw compressor to run in reversed mode. The expander is tested with two working fluids but at a maximum temperature limited to 125 °C. On the other hand, about the twin-screw technology, Smith et al. [19] report a maximum pressure of the fluid at the expander inlet of 25 bar that, considering the working fluid is water, corresponds to a maximum temperature not less than 225 °C.

Ultimately, much higher maximum temperatures are achievable by way of Wankel and reciprocating expanders. They are indeed technologies adapt for internal combustion engines, where temperatures can be remarkably higher than those for the above mentioned technologies. Unlikely Wankel engines, Wankel expanders require though a proper timing mechanism for filling and emptying the working chambers that may be realized via dedicated valves actuated by gears or pulleys [20–22]. Alternatively, a port plate can be adopted, as demonstrated by Badr et al. [23], to control at least the emptying process, which is a solution employed widely in positive-displacement machines for oil-hydraulic applications [24,25]. In their turn, the timing mechanism in reciprocating expanders is realized similarly to reciprocating engines. Despite the potential, reciprocating expander are employed in power generation units, waste heat recovery systems from internal combustion engines, and refrigeration cycles with power requirements of only a few kilowatts and with temperatures in the low range 380–560 °C [1].

1.2. Scope of the work

This work proposes a novel type of expander, named the balanced rolling piston expander, which is a rotary machine with two major characteristics:

1. it can operate at both low and high maximum temperatures of the working fluid, where this high temperature falls between that of a twin-screw and that of a Wankel or reciprocating machine;
2. it does not require any timing mechanism for filling and emptying the working chambers, unlikely Wankel and reciprocating expanders.

As a first investigation of the novel type of expander, the goal of this work is, on the general side, providing the conceptual definition of the balanced rolling piston expander and, on the specific side, verifying the mechanical behavior of a virtual prototype under operational loads. To achieve the later point, a three-step design approach is executed as follows:

1. a geometrical procedure is developed to define the shape of the prototype primary components as well as to compute the velocities and, most importantly, the accelerations of the moving parts (spring-loaded vanes as explained in the next section) during the rotation of the shaft of the prototype itself;
2. a set of thermodynamic laws is utilized to compute the outlet condition of the working fluid, which combined with the previous procedure allows tuning the geometrical parameters to reach a targeted outlet condition;
3. a finite element method analysis of primary components of the prototype is performed to assess their displacements induced by pressure, rotation and temperature.

The following sections of the work present in sequence: the conceptual definition of the novel expander, the design approach as well as the assessment of a virtual prototype, and the conclusions on the feasibility of the expander itself.

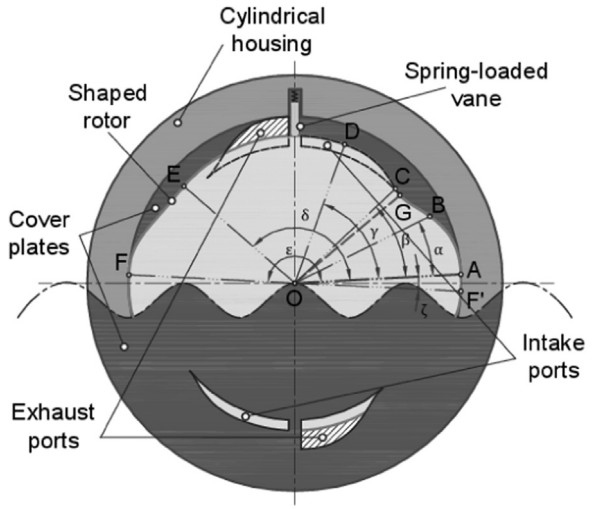

Fig. 1. Schematic of the novel positive-displacement expander, named the balanced rolling piston expander. The primary components are depicted: the cam-shaped rotor, the cylindrical housing with the spring-loaded vane and the cover plates. Moreover, the two intake ports and the two exhaust ports on the back cover plate are also shown.

2. Concept of the balanced rolling piston expander

The balanced rolling piston expander is a rotary machine comprising, as depicted in Fig. 1:

1. one cam-shaped rotor, which is mounted on a shaft;
2. one cylindrical housing, which is coaxial to the rotor;
3. two spring-loaded vanes, which are located in the housing and slide constantly on the rotor flanks providing the sealing between two adjacent working chambers;
4. two cover plates, one of which or even both accommodate the intake and the exhaust ports.

The peculiar shape of the rotor allows for a radially balanced shaft, differently from the common rolling piston architectures [4]. Furthermore, the shape defines four working chambers that vary in volume during the rotation of the rotor. Each cover plate has four ports, two for the intake and two for the exhaust, that have a specific contour matching with the rotor shape for filling and emptying correctly the working chambers. The port locations along the rotation of the rotor define the parameter known as built-in volume ratio, which is for an expander the ratio of the chamber volume at the instant the exhaust port opens and that at the instant the intake port closes. Due to the geometry of the expander, the process is periodical with a period equal to half rotation of the rotor (180°).

The balanced rolling piston expander is proposed for operation at relatively high temperatures of the working fluid because of the extremely limited number of sliding parts: only the two contact points of the vanes with respect to the rotor. Moreover, since lubricating oil is unlikely at high temperatures, the friction at these contact points can be minimized by acting on the load on the vanes or by the use of self-lubricating materials. Two different methods can be used to manufacture the main parts of the expander with self-lubricating materials:

1. synthesizing components by powder metallurgy [26–30], such as for the vanes;
2. spraying the surfaces with coatings [31–35], such as for the rotor and the housing where the vane slides.

Referring to Fig. 2, the operating principle of the machine can be visualized observing two adjacent working chambers, namely I and II, because the processes in the other chambers, III and IV, are specular. The occurring processes are as follows upon half rotation of the rotor.

- The filling process in chamber I starts as the rotor uncovers the intake port and the chamber volume increases (Fig. 2a). The fluid flowing through the intake port allows ideally for a constant-pressure filling. At the same time, the fluid in chamber II is exiting the uncovered exhaust port.
- As soon as the intake port is completely covered (and sealed) by the rotor, the expansion of the fluid in chamber I begins (Fig. 2b). Meanwhile, the fluid in chamber II is continuing to exit the exhaust port.
- The expansion of the fluid in chamber I continues while the emptying process of chamber II is almost completed (Fig. 2c).
- The chamber I reaches the maximum volume, and thus the fluid maximum expansion, while chamber II vanishes (Fig. 2d). At this stage, being the process periodical, a further rotation of the rotor causes the start of both filling the new chamber I, by uncovering its intake port, and the emptying of the old chamber I, which turns into new chamber II, by uncovering its exhaust port. Thus, the

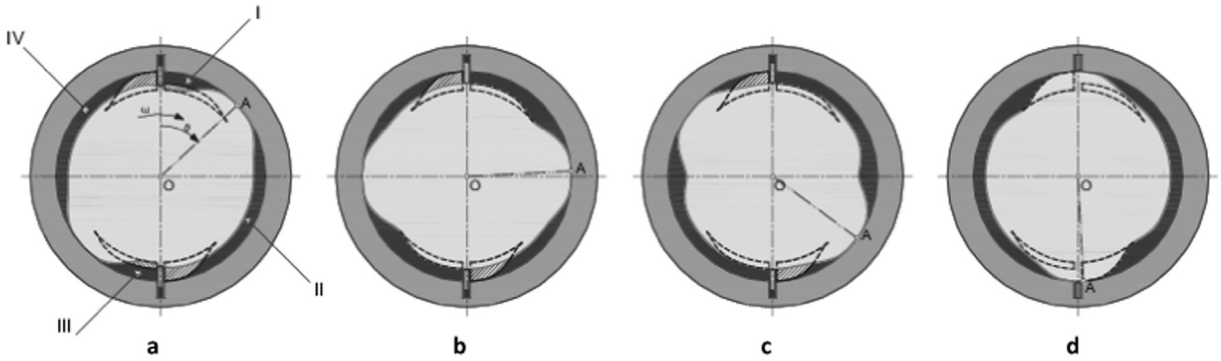

Fig. 2. Schematic of the operating principle and the timing mechanism of the balanced rolling piston expander. From left to right: (a) filling of chamber I, while emptying of chamber II; (b) closing of intake port of chamber I and beginning of expansion in chamber I, while emptying of chamber II continues; (c) expansion continues in both chamber I and II; (d) beginning of emptying of chamber I, while chamber II vanishes. From stage d on, chamber I becomes chamber II and a new chamber I is created. The processes in chambers III and IV are simply specular to the ones in chambers I and II.

process stars over.

The shape of the rotor, which is the key feature of the expander, is generated by a sequence of curves (Fig. 1). Curves AB, BC, CD and EF are described mathematically by polynomials in polar coordinates. Curves AF' and DE are instead circular arcs with center in O. Continuity up to the second order derivative is imposed at every endpoint. Thus, the rotor turns to have a smooth shape to guide properly the vanes. The position of each endpoint of the rotor profile influences strongly the kinematics of the spring-loaded vanes and, consequently, any endpoint must be defined with the goal of avoiding excessive vane accelerations. Most of all, points A and B turn to be crucial because at these points the inertial forces are opposed to the direction of the vane motion. In fact, significant differences between radii OA and OB, along with a small angle α between A and B, may yield high accelerations.

The contour of the intake ports, which is another important feature, is determined considering: externally, the rotor profile, which must completely cover the port at the end of the filling process, and, internally, the circular arc with radius OG. By definition, G is the point on the BC curve of the cam-shaped rotor at which the rotor radius is minimum (Fig. 1). Thus, the point G generates the internal contour of the intake port during its rotation about the center O. The higher the difference between radii OD and OG, the larger the flow passage area for filling the chambers. Analogous design principles are applicable to the contour of the exhaust ports, again with reference to point G as for the internal contour. Lastly, the angular extensions of intake and exhaust ports relate also strictly to the filling and emptying processes of the chambers.

3. Design of the expander

From the geometrical point of view, the proposed expander is a cam-rotor profile. Therefore, the cam-rotor description is

Table 1
Input and output parameters for the design of the balanced rolling piston expander.

Input	Output
Cam-shaped rotor	
Endpoint (A to F) radial coordinates [mm]*	Length of sealing circular arc AF' [mm]
Endpoint (A to F) angular coordinates [rad]*	Polynomial coefficients for curves AB, BC, CD and EF
Cylindrical housing	
	Intake and exhaust port contours and positions
	Inner radius [mm]
	Displaced volume per unit axial length [mm^2]
	Built-in Volume Ratio [-]
	Axial length [mm]
Spring-loaded vanes	
Thickness [mm]	Maximum acceleration [m/s^2]*
	Maximum lift [mm]
Process	
Working fluid	Exhaust pressure [MPa]*
Inlet pressure [MPa]	Exhaust temperature [°C]
Inlet temperature [°C]	Intake volume flow rate [m^3/s]
Mass flow rate [kg/s]	Exhaust volume flow rate [m^3/s]
Rotational speed [rpm]	

* Exhaust pressure is a targeted parameter that is reached by manipulating the endpoint polar coordinates while constraining the maximum vane acceleration.

developed and implemented in a dedicated code following a conventional methodology [36]. As shown on the left column of Table 1, the geometrical procedure takes as main input variables the polar coordinates (i.e. radial and angular coordinates) of the endpoints, A to F, describing the shape of the rotor. These coordinates are uniquely related to the following geometrical characteristics:

- polynomial coefficients for curves AB, BC, CD and EF;
- the sealing circular arc AF';
- the intake and exhaust port contours and positions;
- the inner radius of the housing, which is (approximately) equal to the maximum radius of the rotor (actual dimensions shall take into account clearances and load-induced displacements);
- the displaced volume per unit of axial length, which is the area enclosed by the rotor, the vane and the housing at the instant the intake port closes, as shown in Fig. 2b for chambers I and III;
- the built-in-volume ratio;
- the maximum lift of the vanes, which is equal to the difference between the maximum and the minimum radius of the rotor profile.

Subsequently, the remaining geometrical parameters can be determined via the information on the rotational speed, as shown on the right column of Table 1, such as the maximum vane acceleration that must fall below a threshold and the axial length that allows achieving the desired volume flow rate.

From the thermodynamic point of view, the working fluid is assumed as an ideal gas and the expansion an isentropic process. The pressure drop across the intake port is determined by a nozzle equation imposing constant inlet pressure, temperature and flow rate; in its turn, the pressure drop across the exhaust port is determined in a similar manner. Consequently, the conditions when the exhaust port opens (pressure, temperature and volume flow rate) are determined from the information on the fluid type and on intake conditions (pressure, temperature and mass flow rate) following the mentioned thermodynamic laws. In general, a positive-displacement expander is designed for a targeted exhaust pressure [12], which is strictly related to the built-in volume ratio, in order to avoid fluid-dynamic losses due to over- or under-expansion of the fluid in the working chambers. In the specific case of the balanced rolling piston expander, the polar coordinates of all endpoints are manipulated for the targeted built-in volume ratio, yielding the adapted exhaust pressure, while constraining the maximum acceleration of the vane.

From the structural point of view, the balanced rolling piston expander comprises essentially two primary components: the cam-shaped rotor and the cylindrical housing. These components are subjected to different operational loads. In this design, the assumed loads correspond to the extreme conditions the components may be subjected to during operation, described as follows and visualized by Fig. 3:

- uniform pressure equal to inlet pressure applied on the surface of the components (external surface for the rotor and internal surface for the housing);
- uniform temperature equal to inlet temperature;
- rotational speed equal to maximum speed.

The material for the components shall be chosen considering two issues: the corrosion phenomenon, which is related to the working fluid, and the contact fatigue phenomenon, which is generated by the interaction between the spring-loaded vane and the rotor. Both phenomena can lead to premature failure of the expander [37,38].

The evaluation of the load-induced displacements in the components is performed by the theory of axisymmetric solid [39,40]. This theory is applicable strictly only to the housing, because it is axisymmetric shape, but it can be reasonably extended to the rotor because of its nearly axisymmetric shape. Therefore, the analysis is carried out by the finite element method: the solid models is built in the SOLIDWORKS environment, employing quadratic brick elements, and the numerical analyses is executed by the Simulation package, assuming the mechanical behavior of the material falls in the linear elastic state.

4. Assessment of a virtual prototype

The virtual prototype proposed here is chosen for the study case of a small-scale power generation unit based on a closed-loop Joule-Brayton cycle working with argon, which is a thermodynamic cycle for heat recovery applications currently under investigation [41]. Table 2 defines the adopted parameters for the proposed design. In particular, the vane thickness is taken equal to 6 mm in

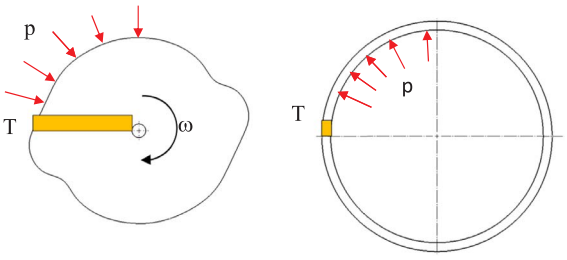

Fig. 3. Main operational loads applied to the cam-shaped rotor as well as to the cylindrical housing of the virtual prototype considered in this work.

Table 2
Assumptions for the analysis of the virtual prototype of the balanced rolling piston expander proposed and simulated in this work.

Input parameter	Unit	Value
Geometrical data		
Polar coordinates (radial / angular)		
Endpoint A	mm/deg	120 / 2.9
Endpoint B	mm/deg	108.8 / 26.2
Endpoint C	mm/deg	99.6 / 43.1
Endpoint D	mm/deg	106.3 / 70.1
Endpoint E	mm/deg	106.3 / 138.8
Endpoint F	mm/deg	120 / 177.1
Vane thickness	mm	6
Thermodynamic data		
Working fluid		argon
Inlet pressure	MPa	1.35
Inlet temperature	°C	500
Mass flow rate	g/s	115
Rotational speed	rpm	1000
Finite element method analysis		
Type of elements		quadratic brick
Number of elements (rotor and housing)		30,000
Reference temperature	°C	500
Material		Stainless steel
Young modulus	MPa	170,000
Poisson modulus		0.3
Tangential elastic modulus	MPa	63,500
Linear thermal expansion coefficient	K^{-1}	$1.8\ 10^{-5}$

symmetry with the thickness of the machine described by Jiang et al. [42], which is similar to the proposed expander but it is not radially balanced.

After generating the rotor profile, based on the assumptions from Table 2, the rotor and housing shapes are exported into the AutoCAD environment where chamber areas, i.e. volumes per fixed axial length, are calculated by the software for a number of rotor positions. The exhaust port is positioned to achieve a desired built-in volume ratio of 2.3, which is a value resulting from the optimization of the investigated heat recovery cycle [41].

Given the specific heat ratio of 1.67 for argon and the inlet pressure and temperature (Table 2) as well as considering an isentropic expansion, the pressure expansion ratio when the exhaust port opens is $2.3^{1.67} = 4$ and, hence, the fluid conditions are 0.34 MPa and 158 °C. These calculations are justified under the assumption of no fluid leakage throughout the process, as conventionally adopted in the preliminary study of positive-displacement expanders [12].

The resulting axial length and ideal power output are 100 mm and 20 kW (see Appendix A for calculations). These important results provide an indication of the output capacity of the machine with respect to its geometrical size, but the real power output shall be expected to be appreciably lower. In general, the expander efficiency depends on the actual value of the expansion ratio, the effects of heat transfers, the mechanical friction losses, the throttling at the intake port, and the leakage flow rates [12]. Although the calculation of the expansion efficiency lies outside the scope of the present research, the isentropic efficiency of the proposed expander is expected to exceed the value reported in literature (50–60%) for sliding-vane architectures [1,2,5–11], at even higher maximum temperatures, thanks to the extremely limited number of sliding parts and to the reduced number of working chambers.

Fig. 4 shows the lift and the acceleration of the vane as functions of the rotation angle (in agreement with Fig. 2, the segment OA is taken as the reference for the angle). In particular, the vane acceleration can reach relatively high values that are anyhow

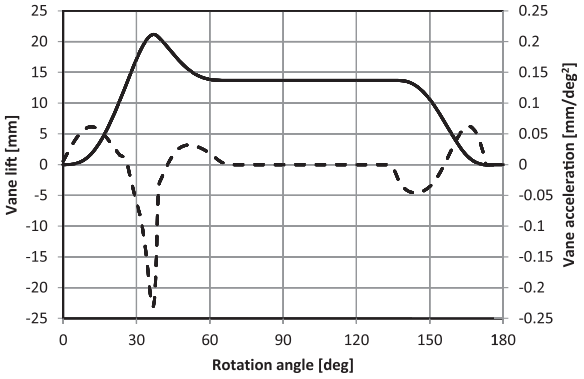

Fig. 4. Vane lift (solid line) and vane acceleration (dashed line) for the virtual prototype.

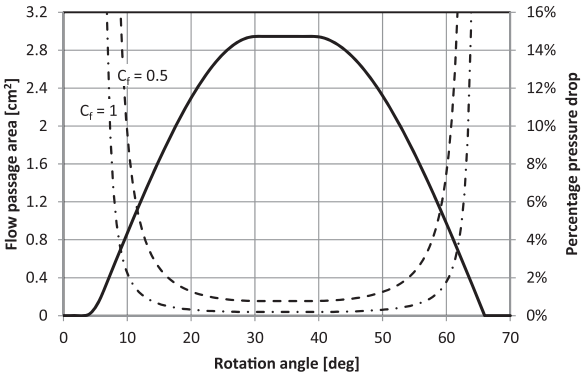

Fig. 5. Flow passage (solid line) area and percentage pressure drops for two discharge coefficients, indicated by C_f, at the intake (dashed lines). Percent pressure drop is defined with respect to the supply pressure. The discharge coefficient equal to 1 refers to the ideal case.

comparable to those of sliding vane machines of similar size. Maximum vane acceleration shall be used in a next stage for calculating the inertial forces and for sizing the springs loading the vanes. Moreover, Fig. 5 visualizes the fluid throttling through the intake port (Fig. 1) as a function of the rotation angle for two discharge coefficients: the first equal to 1, which is the ideal case, and the other to 0.5, which is considered a more realistic case. As soon as the port is uncovered or just before it is covered by the rotor, pressure drops can reach fairly high values in percent terms; however, they decrease rapidly close to 1% away from those two angular positions. Nonetheless, percent pressure drops can be lowered simply duplicating the intake ports also on the second cover plate. Pressure drops across the exhaust port are similar to those in Fig. 5, but much lower in magnitude thanks to a larger passage area (Fig. 1).

Fig. 6 depicts the results of the finite element analysis imposing the operational loads, singularly and collectively, to the rotor. The displacement induced on the rotor by pressure is $5.6{\cdot}10^{-4}$ mm (Fig. 6a), by rotation is $1.3{\cdot}10^{-4}$ mm (Fig. 6b), and by temperature as well as by all loads is 0.754 mm (Fig. 6c). Hence, temperature turns to be the only load inducing appreciable displacements on the rotor. Likewise, Fig. 7 depicts the results imposing collectively the loads to the cylindrical housing for two thicknesses: the first of 10 mm and the other of 50 mm. The induced displacement on the inner radius of the housing is 0.749 mm in both cases. Ultimately, the induced interference between rotor and housing when subjected to all loads is about 0.005 mm. This load-induced interference shall be used for determining the actual radial clearance between rotor and housing at room temperature.

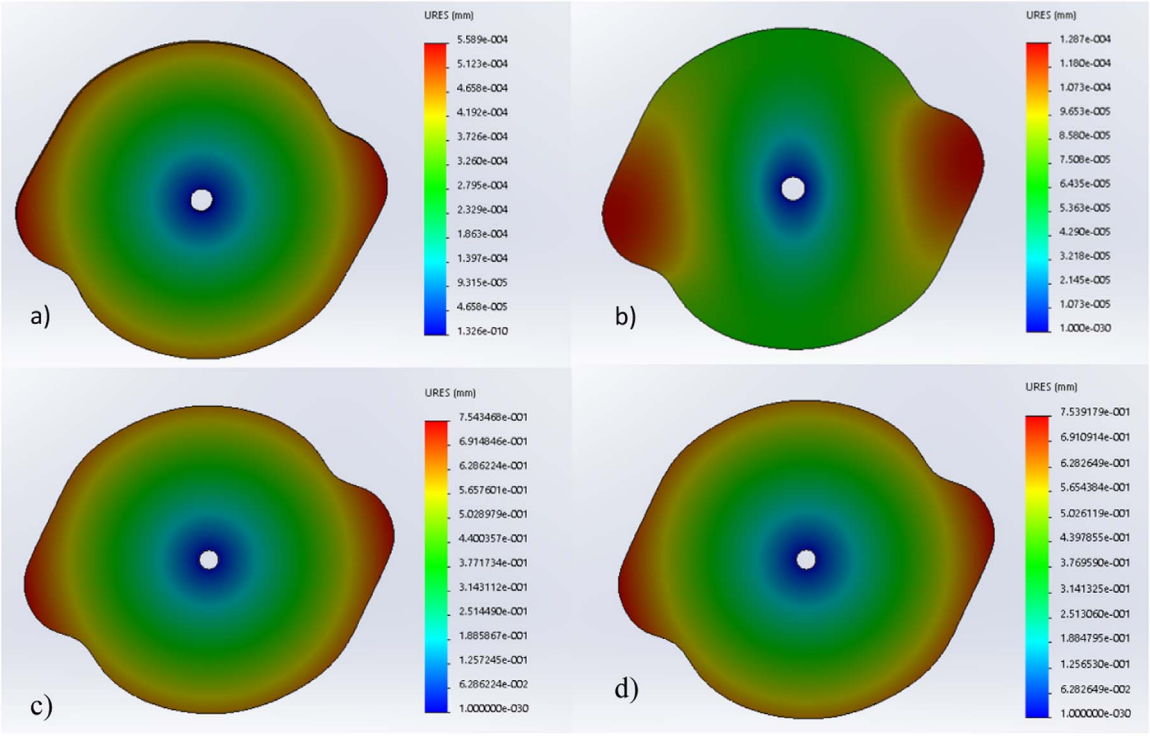

Fig. 6. Rotor displacement in [mm], for different operational load applied singularly: a) uniform pressure of 13.5 bar; b) rotation at 1000 rpm; c) uniform temperature at 500 °C, and d) the displacement results for all this load applied to the component.

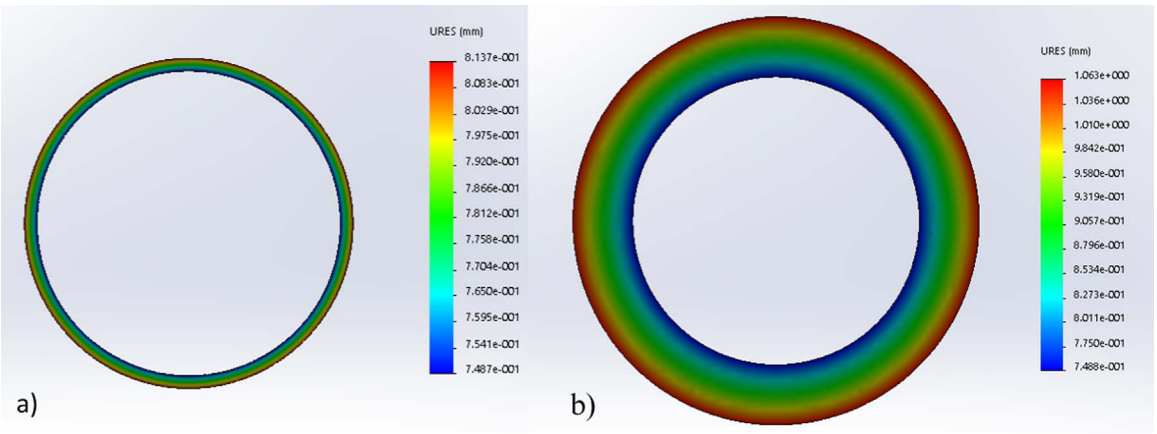

Fig. 7. Housing displacement in [mm] subjected all operation loads: a) thickness of 10 mm; b) thickness of 50 mm.

5. Conclusions

This work presents a novel type of positive-displacement expander, named the balanced rolling piston expander. It proposes also a design procedure and it assesses the mechanical behavior of a virtual prototype. This prototype is chosen for the study case of a small-scale heat recovery unit, based on a closed-loop Joule-Brayton cycle currently under investigation. The conclusions of the work are as follows.

- The virtual prototype, which is bulkily a cylinder with diameter of around 300 mm and a length of 100 mm, is capable of generating an ideal power output of 20 kW under the study case conditions.
- Vane accelerations can reach relatively high values, which shall be handled by loading springs, but those values are anyhow comparable to sliding vane machines of similar size.
- Pressure drops, in percent terms, across intake and exhaust ports, which vary during the rotation of the rotor, are most of the rotation close to 1%, for the case of the intake, and even lower, for the exhaust.
- Displacement induced onto the rotor and the housing by the operational loads of the study case are lower than 1 mm and yielded interferences between this components shall be managed by a small radial clearance at room temperature.

In brief, the balanced rolling piston expander appears to be a promising option for small-scale power generation units operating with temperatures not achievable by common technologies and, hence, it deserves further investigation.

Appendix A

This section reports the calculation of the ideal power output from the expander, P_{id} [W], as the product between the mass flow rate $\dot{m}$ [kg/s], which is an input design parameter, and the ideal specific work, w_{id} [J/kg]:

$$P_{id} = \dot{m} \bullet w_{id} \tag{A1}$$

In its turn, the specific work w_{id} is related to the fluid specific heat ratio k [-], inlet pressure p_{in} [Pa], outlet pressure, p_{out} [Pa], and specific volume, v_{in} [m^3/kg], as well as it is related to the pressure ratio, which depends ultimately on the fixed built-in volume ratio, bvr [-]:

$$w_{id} = \frac{k}{k-1} \bullet p_{in} \bullet v_{in} \bullet \left[1 - \left(\frac{p_{out}}{p_{in}} \right)^{\frac{k-1}{k}} \right] = \frac{k}{k-1} \bullet p_{in} \bullet v_{in} \bullet \left[1 - \left(\frac{1}{bvr} \right)^{k-1} \right] \tag{A2}$$

Based on the calculation assumptions, the specific work is around 170 kJ/kg and, hence, the ideal power output about 20 kW.

References

[1] M. Imran, M. Usman, B.S. Park, D.H. Lee, Volumetric expanders for low grade heat and waste heat recovery applications, Renew. Sustain. Energy Rev. 57 (2016) 1090–1109.
[2] J. Bao, L. Zhao, A review of working fluid and expander selections for organic Rankine cycle, Renew. Sustain. Energy Rev. 24 (2013) 325–342.
[3] G. Haiqing, M. Yitai, L. Minxia, Some design features of CO_2 swing piston expander, Appl. Therm. Eng. 26 (2006) 237–243.
[4] N. Zheng, L. Zhao, X.D. Wang, Y.T. Tan, Experimental verification of a rolling-piston expander that applied for low-temperature Organic Rankine Cycle, Appl. Energy 112 (2013) 1265–1274.
[5] G. Qiu, H. Liu, S. Riffat, Expanders for micro-CHP systems with organic Rankine cycle, Appl. Therm. Eng. 31 (2011) 3301–3307.

[6] O. Badr, P.W. O'Callaghan, S.D. Probert, Multi-vane expanders: geometry and vane kinematics, Appl. Energy 19 (1985) 159–182.
[7] O. Badr, S.D. Probert, P.W. O'Callaghan, Performances of multi-vane expanders, Appl. Energy 20 (1985) 207–234.
[8] H. Liu, G. Qiu, F. Daminabo, Y.J. Shao, S.B. Riffat, Preliminary experimental investigations of a biomass-fired micro-scale CHP with organic Rankine cycle, Int. J. Low Carbon Technol. 5 (2010) 81–87.
[9] R. Cipollone, G. Bianchi, D. Di Battista, G. Contaldi, S. Murgia, Mechanical energy recovery from low grade thermal energy sources, Energy Procedia 45 (2014) 121–130.
[10] Z. Gnutek, P. Kolasinski, The application of rotary vane expanders in organic Rankine cycle systems - Thermodynamic description and experimental results, J. Eng. Gas. Turbines Power 135 (6) (2013) (no.061901).
[11] M. Farrokhi, S.H. Noie, A.A. Akbarzadeh, Preliminary experimental investigation of a natural gas-fired ORC-based micro-CHP system for residential buildings, Appl. Therm. Eng. 69 (2014) 221–229.
[12] V. Lemort, S. Quoilin, C. Cuevas, J. Lebrun, Testing and modeling a scroll expander integrated into an organic Rankine cycle, Appl. Therm. Eng. 29 (2009) 3094–3102.
[13] S. Declaye, S. Quoilin, L. Guillaume, V. Lemort, Experimental study on an open-drive scroll expander integrated into an ORC (Organic Rankine Cycle) system with R245fa as working fluid, Energy 55 (2013) 173–183.
[14] A. Giuffrida, Modelling the performance of a scroll expander for small organic Rankine cycles when changing the working fluid, Appl. Therm. Eng. 70 (1) (2014) 1040–1049.
[15] S. Quoilin, V. Lemort, J. Lebrun, Experimental study and modeling of an organic Rankine cycle using scroll expander, Appl. Energy 87 (2010) 1260–1268.
[16] R.B. Peterson, H. Wang, T. Herron, Performance of a small-scale regenerative Rankine power cycle employing a scroll expander proceedings of the institution of mechanical engineers, Part A J. Power Energy 222 (3) (2008) 271–282.
[17] V. Lemort, S. Declaye, S. Quoilin, Experimental characterization of a hermetic scroll expander for use in a micro-scale Rankine cycle proceedings of the institution of mechanical engineers, Part A J. Power Energy 226 (1) (2012) 126–136.
[18] A. Desideri, S. Gusev, M. van den Broek, V. Lemort, S. Quoilin, Experimental comparison of organic fluids for low temperature ORC (organic Rankine cycle) applications, Energy 97 (2016) 460–469.
[19] I.K. Smith, N. Stosic, E. Mujic, A. Kovacevic, Steam as the working fluid for power recovery from exhaust gases by means of screw expanders proceedings of the institution of mechanical engineers, Part E J. Process Mech. Eng. 225 (2) (2011) 117–125.
[20] O. Badr, S. Naik, P.W. O'Callaghan, S.D. Probert, Rotary wankel engines as expansion devices in steam Rankine-cycle engines, Appl. Energy 39 (1991) 59–76.
[21] M. Antonelli, L. Martorano, A study on the rotary steam engine for distributed generation in small size power plants, Appl. Energy 97 (2012) 642–647.
[22] M. Antonelli, A. Baccioli, M. Francesconi, U. Desideri, L. Martorano, Operating maps of a rotary engine used as an expander for micro-generation with various working fluids, Appl. Energy 113 (2014) 742–750.
[23] O. Badr, S. Naik, P.W. O'Callaghan, S.D. Probert, Wankel engines as steam expanders: design considerations, Appl. Energy 40 (1991) 157–170.
[24] A. Giuffrida, R. Lanzafame Modeling and simulation of a balanced vane pump, in: Proceedings of the 2001 ASME IMECE - Fluid Power Systems and Technology, New York, USA, 11–16 November 2001.
[25] A. Giuffrida, R. Lanzafame, Cam shape and theoretical flow rate in balanced vane pumps, Mech. Mach. Theory 40 (2005) 353–369.
[26] S. Zhu, Q. Bi, J. Yang, W. Liu, Q. Xue, Ni_3Al matrix high temperature self-lubricating composites, Tribology Int. 44 (4) (2011) 445–453.
[27] C. Dellacorte, H.E. Slinet, M.S. Bogdanski, Tribological and mechanical comparison of sintered and HIPped PM212: high temperature self-lubricating composites, Lubr. Eng. 48 (11) (1992) 877–885.
[28] Y. Solmaz, M.H. Kelestemur, Wear behaviour of boron-doped Ni_3Al material at elevated temperature, Wear 257 (9–10) (2004) 1015–1021.
[29] J. Han, J. Jia, J. Lu, J. Wang, High temperature tribological characteristics of Fe-Mo based self-lubricating composites, Tribology Lett. 34 (3) (2009) 193–200.
[30] J. Wang, y. Shan, H. Guo, B. Li, W. Wang, J. Jia, Friction and wear characteristics of hot–pressed NiCrMo/MoO_3/Ag Self-lubrication composite at elevated Temperature up to 900 °C, Tribology Lett. 59 (3) (2015) 48.
[31] C. Petrogalli, L. Montesano, M. Gelfi, G.M. La Vecchia, L. Solazzi, Tribological and corrosion behaviour of CrN coatings: roles of substrate and deposition defects, Surf. Coat. Technol. 258 (2014) 878–885.
[32] W. Wang, Application of a high temperature self-lubrication composite coating on steam turbine components, Surf. Coat. Technol. 177–178 (2004) 12–17.
[33] T. Zhang, H. Lan, C. Huang, S. Yu, L. Du, W. Zhang, Preparation and characterizations of nickel – based composite coatings with self-lubricating property at elevated temperature, Surf. Coat. Technol. 294 (2016) 21–29.
[34] Z. Xu, X. Shi, Q. Zhang, W. Zhai, X. Li, J. Yao, S. Song, L. Chen, Y. Xiao, Q. Zhu, Wear and friction of TiAl matrix self-lubricating composites against Si_3N_4 in air at room and elevated temperature, Tribology Trans. 57 (6) (2014) 1017–1027.
[35] X. Deng, X. Shi, X. Liu, Y. Huang, Z. Yan, K. Yang, Y. Wang, Effect of Ti_3SiC_2 on tribological properties of M50 matrix self –lubrication composites from 25 to 450 °C, J. Mater. Eng. Perform. 26 (9) (2017) 4595–4604.
[36] F.Y. Chen, Mechanics and Design of Cam Mechanisms, Pergamon Press, New York, 1982.
[37] L. Solazzi, R. Scalmana, M. Gelfi, G.M. Vecchia, Effect of different corrosion level an mechanical behavior and failure of threaded elements, J. Fail. Anal. Prev. 12 (2012) 541–549.
[38] L. Solazzi, C. Petrogalli, M. Lancini, Vibration based diagnostic on rolling contact fatigue test bench, Procedia Eng. 10 (2011) 3465–3470.
[39] sP. Timoschenko, J.N. Goodier, Theory of Elasticity, McGraw-Hill, 1987.
[40] A.P. Boresi, K.P. Chong, J.D. Lee, Elasticity in Engineering Mechanics, John Willey & Sons, 2011.
[41] G. Valenti, A. Valenti, C. Valenti, Method and System for Converting Thermal Power, Delivered from A Variable Temperature Heat Source into Mechanical Power. PCT application. 〈http://patentscope.wipo.int/search/en/WO2012063275〉.
[42] Y. Jiang, Y. Ma, L. Fu, M. Li, Some design features of CO_2 two-rolling piston expander, Energy 55 (2013) 916–924.